Earth and Planetary Science Letters 427 (2015) 249–261

Contents lists available at ScienceDirect

Earth and Planetary Science Letters

www.elsevier.com/locate/epsl

Constraints on the accretion of the gabbroic lower oceanic crust from plagioclase lattice preferred orientation in the Samail ophiolite

J.A. VanTongeren [a,*], G. Hirth [b], P.B. Kelemen [c]

[a] Department of Earth and Planetary Sciences, Rutgers University, 610 Taylor Rd., Piscataway NJ 08854, United States
[b] Department of Earth, Environmental, and Planetary Sciences, Brown University, 324 Brook St. Providence, RI 02912, United States
[c] Department of Earth and Environmental Sciences, Columbia University, 557 Schermerhorn Extension, New York, NY 10027, United States

ARTICLE INFO

Article history:
Received 26 February 2015
Received in revised form 30 June 2015
Accepted 1 July 2015
Available online 24 July 2015
Editor: T.A. Mather

Keywords:
lower oceanic crust
plagioclase LPO
Samail ophiolite
Oman

ABSTRACT

Oceanic crust represents more than 60% of the earth's surface and despite a large body of knowledge regarding the formation and chemistry of the extrusive upper oceanic crust, there still remains significant debate over how the intrusive gabbroic lower oceanic crust is accreted at the ridge axis. The two proposed end-member models, the Gabbro Glacier and the Sheeted Sills, predict radically different strain accumulation in the lower crust during accretion. In order to determine which of these two hypotheses is most applicable to a well-studied lower crustal section, we present data on plagioclase lattice preferred orientations (LPO) in the Wadi Khafifah section of the Samail ophiolite. We observe no systematic change in the strength of the plagioclase LPO with height above the crust-mantle transition, no dominant orientation of the plagioclase a-axis lineation, and no systematic change in the obliquity of the plagioclase LPO with respect to the modal layering and macroscopic foliation evident in outcrop. These observations are most consistent with the Sheeted Sills hypothesis, in which gabbros are crystallized *in situ* and fabrics are dominated by compaction and localized extension rather than by systematically increasing shear strain with increasing depth in a Gabbro Glacier. Our data support the hypothesis of MacLeod and Yaouancq (2000) that the rotation of the outcrop-scale layering from sub-horizontal in the layered gabbros to sub-vertical near the sheeted dikes is due to rapid vertical melt migration through upper gabbros close to the axial magma chamber. Additionally, our results support the hypothesis that the majority of extensional strain in fast spreading ridges is accommodated in partially molten regions at the ridge axis, whereas in slow and ultra-slow ridges large shear strains are accommodated by plastic deformation.

1. Introduction

Over the last half-century significant progress has been made in seismic imaging of active fast-intermediate spreading mid-ocean ridges. Detailed 2D and 3D profiles of the mid-ocean ridge axis at the East Pacific Rise (EPR) and Juan de Fuca Ridge have revealed the occurrence and geometry of the shallow axial magma chamber (AMC) in high resolution (Detrick et al., 1987; Singh et al., 1998; Han et al., 2014). In addition, scientific ocean drilling has provided an important tool for understanding the petrology and geochemistry of gabbroic rocks inferred to have crystallized in the AMC, and their relationship to the overlying extrusive basalts (e.g., Gillis et al., 1993; Teagle et al., 2012). One important feature of the global mid-ocean ridge system, however, remains uncertain: the mechanism of accretion of gabbroic lower oceanic crust. Recently, IODP Expedition 345 recovered 110 meters of drill core sampling tectonically exposed, gabbroic lower crust at three sites in Hess Deep (Gillis et al., 2014). The core recovered on this expedition represents the best *in situ* sampling available, however the original "stratigraphic" depth represented remains uncertain. Thus, ophiolites, and especially the Samail ophiolite of Oman and the United Arab Emirates, offer the best-constrained examples of lower crust formed at submarine spreading centers.

Two end-member hypotheses for the formation and accretion of the lower crust at spreading ridges emerged in the 1990s, together with many options intermediate between these end-members (Fig. 1). The "Gabbro Glacier" hypothesis is that crystallization occurs primarily in the seismically-imaged AMC at the base of the sheeted dikes, and the lower crust is built by viscous flow of these cumulates downward and outward, away from the spreading center (Sinton and Detrick, 1992; Sleep, 1975; Phipps Morgan and Chen, 1993; Henstock et al., 1993;

* Corresponding author.
E-mail address: jvantongeren@eps.rutgers.edu (J.A. VanTongeren).

http://dx.doi.org/10.1016/j.epsl.2015.07.001

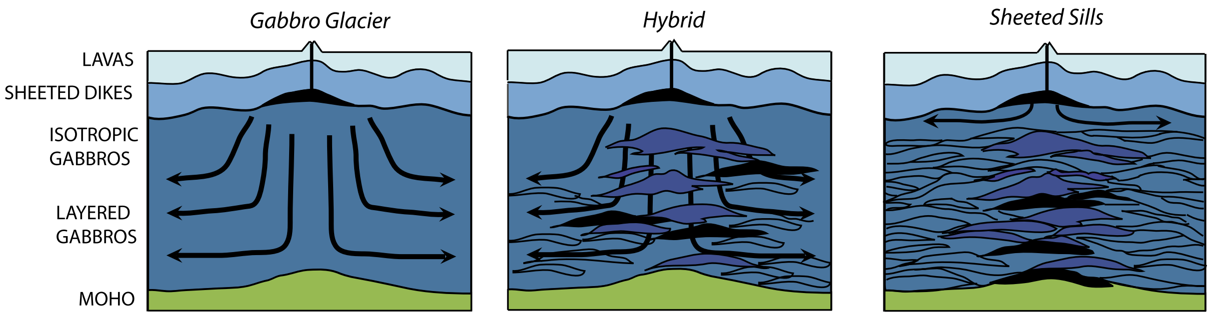

Fig. 1. Illustration of the Gabbro Glacier (e.g., Sinton and Detrick, 1992; Sleep, 1975; Morgan and Chen, 1993; Henstock et al., 1993; Quick and Denlinger, 1993), Hybrid (e.g. Boudier et al., 1996), and Sheeted Sills (e.g. Kelemen et al., 1997; Korenaga and Kelemen, 1998) mechanisms for lower crustal accretion at intermediate-fast spreading ridges. It is important to note that the Sheeted Sills end-member depicted here, and envisioned by Korenaga and Kelemen (1998), includes a small Gabbro Glacier directly beneath the sheeted dikes and a lower crust entirely accreted by small sills; whereas, the Hybrid model of Boudier et al. (1996) envisions a crustal scale Gabbro Glacier into which small sills are periodically emplaced.

Quick and Denlinger, 1993). By contrast, the "Sheeted Sills" hypothesis is that the lower crust is accreted in a series of small sills that are emplaced and crystallized *in situ* at the crustal depth where they are currently found (Kelemen et al., 1997; Korenaga and Kelemen, 1998; Boudier et al., 1996).

The Sheeted Sills hypothesis requires efficient extraction of thermal energy from the entire crustal section near the spreading ridge, in order to account for near-ridge crystallization of gabbroic rocks at the base of the crust (e.g., Maclennan et al., 2004). This implies that igneous and high temperature metamorphic cooling rates are rapid near the axis of the spreading center. Results from measured cooling rates in the Samail ophiolite are mixed: Coogan et al. (2002) used Ca diffusion in olivine to infer slow cooling rates for the anomalously thin Wadi Al Abyad crustal section. In contrast, Garrido et al. (2001) and VanTongeren et al. (2008) inferred rapid cooling rates for the thicker, Wadi Khafifah section on the basis of crystal size distributions and Ca diffusion in olivine, respectively. VanTongeren et al. (2008) suggested that cooling in the Wadi Al Abyad section might have been extended during a long period of off-axis magmatism, since the mantle section there is intruded by swarms of medium- to fine-grained gabbroic dikes.

A more direct way to distinguish between the products of the Sheeted Sill versus Gabbro Glacier mechanisms is to constrain the kinematic evolution of gabbro cumulates as a function of depth below the paleo-AMC (Fig. 2). Whereas the Sheeted Sill process is not likely to produce systematic variation in strain with depth in the crust, the Gabbro Glacier mechanism requires increasing shear strain as well as a rotation of the shear plane with increasing depth below the AMC (Fig. 2).

In this study we present data on plagioclase lattice preferred orientations (LPOs) in gabbros from a detailed section through the lower crust of the Samail ophiolite. Plagioclase comprises 45–65 volume percent of all of our samples. The strength, geometry, and orientation of the plagioclase fabric provides a record of the strain history experienced during rock formation and can be used to distinguish between crustal sections formed by the Gabbro Glacier versus Sheeted Sills mechanisms.

2. Background

2.1. Gabbro glacier vs. sheeted sills

In the Gabbro Glacier mechanism, the entire lower crust (∼4–5 km of gabbroic cumulates) crystallizes within a ∼50–100 thick AMC located below the sheeted dikes, and the lower crust forms by subsidence and magmatic flow downward from the AMC and laterally away from the spreading center axis (Sinton and Detrick, 1992; Quick and Denlinger, 1993). This hypothesis was originally conceived to incorporate crustal accretion in a simple model of heat budget for spreading centers (Sleep, 1975) and was proposed to be consistent with three main observations: First, in the Samail ophiolite, the outcrop-scale layering in the gabbros evolves from Moho-parallel near the base of the crust to dike-parallel near the paleo-AMC (Pallister and Hopson, 1981; Smewing, 1981; Nicolas et al., 1988a; 2009). Second, prior to recent seismic experiments showing off-axis melt lenses (Han et al., 2014; Canales et al., 2006; 2009) and Moho-level reflectors, (Singh et al., 2006), the AMC was the only laterally persistent magma chamber that had been imaged seismically at active spreading centers, such as the EPR. A recent multichannel seismic study of the EPR, however, shows clear evidence of several sub-axial melt lenses throughout the lower crust (Marjanović et al., 2014). Third, early numerical models of lower crustal accretion assumed that hydrothermal circulation did not occur in rocks above 600 °C (Lister, 1977). This assumption translated into thermal profiles of the oceanic crust in excess of 1000 °C as much as 4 km off-axis near the Moho (Morgan and Chen, 1993; Chen, 2001). Under these circumstances, crystallization is expected to be most efficient in the shallow AMC where active hydrothermal circulation can effectively advect heat away from the magma chamber (e.g. Lister, 1977). The assumption of a cap at 600 °C is likely incorrect as high-temperature (750–950 °C) alteration phases such as pargasite and chlorite are present in gabbros near the Moho in the exposed sections of the Samail ophiolite (Manning et al., 2000; Bosch et al., 2004) and in gabbros from Hess Deep (Mevel et al., 1996).

We reiterate that Ca-in-olivine speedometry in one of two crustal sections analyzed so far yields fast cooling rates through the ∼800 °C isotherm extending down to the Moho, without systematic variation with depth (VanTongeren et al., 2008). The fast cooling rates are also supported by ages and cooling rates of zircons found at slow-spreading mid-ocean ridges such the Mid-Atlantic and Southwest Indian ridges (Grimes et al., 2011; Rioux et al., 2012; Schmitt et al., 2011), as well as heat flow studies (Spinelli and Harris, 2011), and interpretation of steep contours of seismic P-wave speeds as indicating nearly vertical isotherms in the lower crust at the EPR (Dunn et al., 2000).

The thermal profile of the crust determined by the cooling rates, and modeled numerically with active hydrothermal circulation (Cherkaoui et al., 2003; Maclennan et al., 2004) suggests that *in situ* crystallization of individual melt lenses deep in the crust may be possible at or near the ridge-axis, regardless of the depth of intrusion below the sheeted dikes – as is proposed in the Sheeted Sills hypothesis. Other evidence in support of the Sheeted Sills hypothesis includes: (1) the presence of meter to centimeter-scale cryptic variation in lower gabbro geochemistry (Browning, 1984) suggesting differentiation *in situ* without any significant reorganization of the cumulate pile; (2) observed modally graded layering in the lower gabbros (e.g., Pallister and Hopson, 1981) that

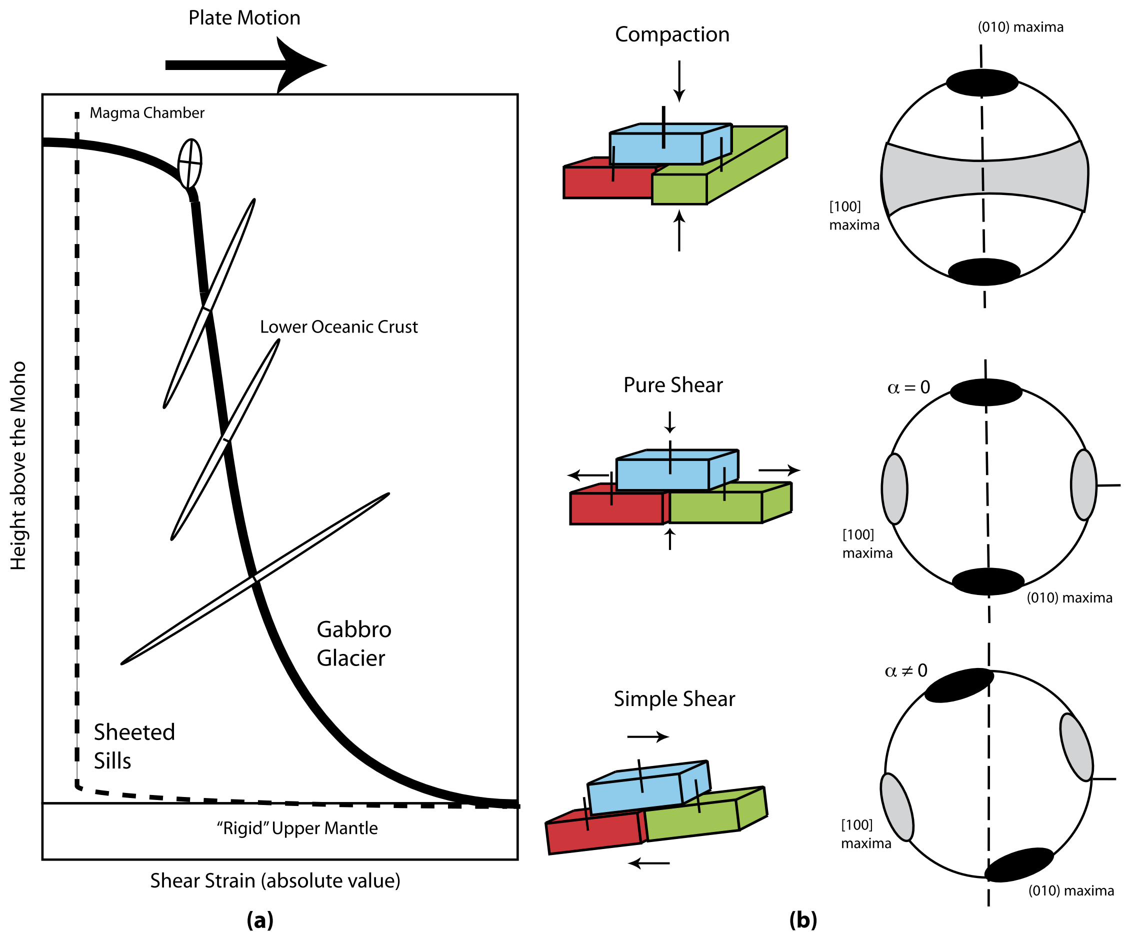

Fig. 2. (a) Schematic prediction of strain in the Gabbro Glacier (solid black line) and Sheeted Sills (dashed line) mechanisms. The prediction of strain for the Gabbro Glacier mechanism is based on the calculations of Phipps Morgan and Chen (1993). Strain ellipses illustrate the rotation of the shear plane due to the vertical component of flow in the Gabbro Glacier setting, as quantified in Fig. 4 of Phipps Morgan and Chen (1993). Also see Quick and Denlinger (1993). (b) Response of plagioclase fabrics to compaction, pure shear, and simple shear based on the experiments of Benn and Allard (1989), Ildefonse et al. (1992a, 1992b), Picard et al. (2011). Black circles indicate the location of the b-axis maxima. Gray regions indicate the location of the a-axis maxima. α is the obliquity between the plagioclase b-axis maxima and the pole to the compositional layering.

would likely not survive the shear strain associated with ductile flow in the Gabbro Glacier (Korenaga and Kelemen, 1998), though recent work by Jousselin et al. (2012) has questioned this interpretation; (3) seismic velocity and compliance measurements from the EPR indicating the presence of significant volumes of melt at specific horizons in the lower crust (Crawford and Webb, 2002; Zha et al., 2014).

2.2. Predicted strain in the Gabbro Glacier and Sheeted Sills hypotheses

The Gabbro Glacier and Sheeted Sills hypotheses entail very different evolution of accumulated strain with depth below the AMC. In the Sheeted Sills hypothesis, gabbros formed *in situ* experience volumetric strain via compaction, as well as local pure or simple shear. Additionally, in the Sheeted Sills scenario, there should be no systematic change in fabric strength or strain magnitude with depth (Fig. 2a). In contrast, in the Gabbro Glacier hypothesis, the gabbroic cumulates are expected to be deformed both vertically (by downward advection of gabbros below the AMC) and laterally (by the motion of the crust away from the ridge axis) (e.g. Quick and Denlinger, 1993; Phipps Morgan and Chen, 1993; Nicolas et al., 2009), resulting in extreme shear strain in the lowermost portions of the crust near the Moho.

2.3. Interpretation of plagioclase fabrics

Plagioclase has triclinic crystal symmetry and its LPO can be described by the [100] axis and poles to (010) and (001) planes. Because plagioclase crystals often have a large aspect ratio, with crystals being significantly longer along [100] than along (010) or (001), plagioclase shape fabrics are correlated with the LPO during suprasolidus deformation making both shape fabrics and LPO in plagioclase potentially excellent recorders of crystal alignment and strain in gabbroic rocks.

During compaction, the shortest dimension of the plagioclase grains, typically parallel to the b-axis [010], aligns parallel to the direction of maximum compressional strain (e.g. vertical for a sill parallel to the Moho and the seafloor; Benn and Allard, 1989; Ildefonse et al., 1992a, 1992b). The long axis, the a-axis [100] will align perpendicular to the pole to (010), and the poles to (001) show a weaker LPO. On pole figures, compaction is manifest as a point maximum in poles to (010), and a girdle in [100] (Fig. 2b). During pure shear, the plagioclase [100] axis will align parallel to the direction of extension or flow (Benn and Allard, 1989; Ildefonse et al., 1992a, 1992b) resulting in pole figures with [100] point maxima. During simple shear, plagioclase pole figures will display point maxima in both poles to (010) and [100] oblique to both the macroscopic foliation and the shear plane, and a central point maxima in poles to (001) (Ildefonse et al., 1992a;

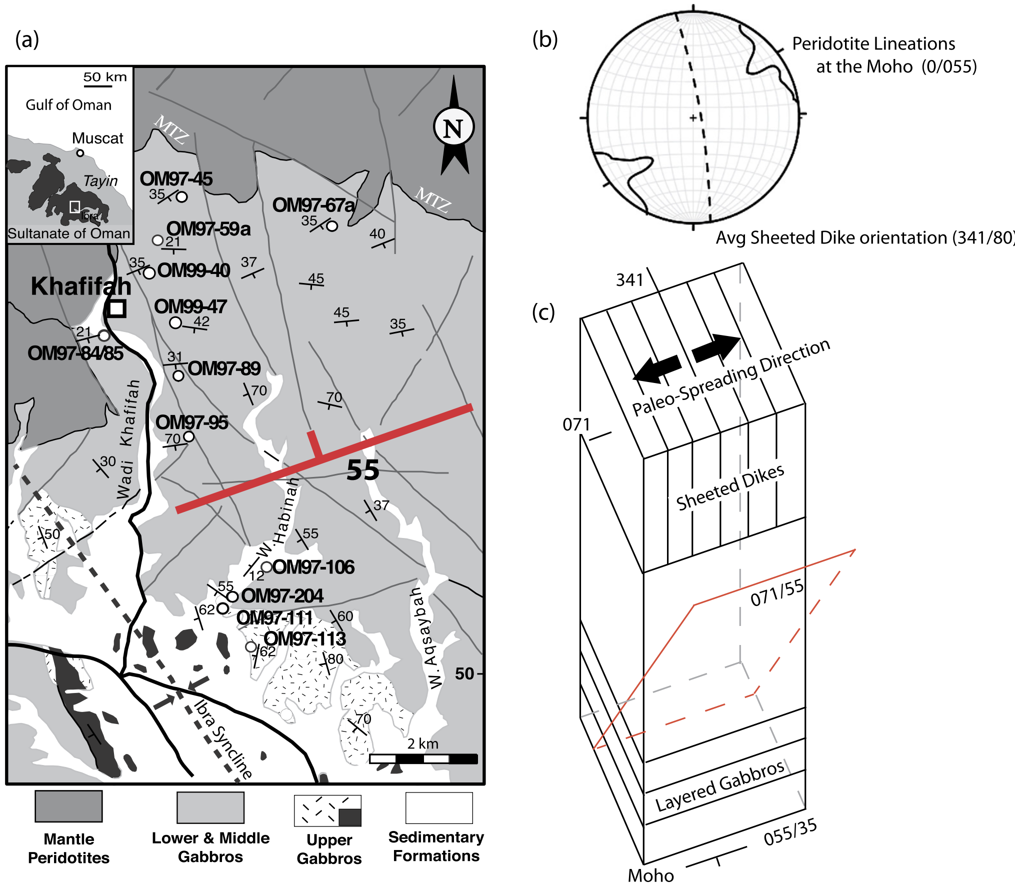

Fig. 3. (a) Map of the Wadi Khafifah sampling locations in the Samail ophiolite adapted from Garrido et al. (2001) and the location of the Ibra Syncline as mapped by Pallister and Hopson (1981). Large red orientation line is the strike (071) and dip (55°) of the geographic reference frame (see text). Small map inset shows the location of our sampling region relative to the Samail and Wadi Tayin massifs of the Oman ophiolite; areas of exposed outcrop shown in black. (b) Orientation of the sheeted dikes and Moho lineations in the Wadi Khafifah region from Nicolas et al. (1988a). It is important to note that the Moho and sheeted dikes in this region are not perpendicular to one other, the Moho is approximately 60–70° oblique to the sheeted dikes. (c) 3D crustal column illustrating the choice of geographic reference frame (red plane). All samples were rotated into the geographic reference frame, which is a plane perpendicular to both the paleo-spreading direction and the compositional layering. (For interpretation of the references to color in this figure legend, the reader is referred to the web version of this article.)

Picard et al., 2011; Fig. 2b). The obliquity evolves with increasing shear strain, depending on the aspect ratio of the grains and if deformation also involves a component of pure shear (e.g., Ghosh and Ramberg, 1976). At high shear strains, on the order of 5–10, the [100] maxima can become aligned subparallel to the shear direction.

Due to the anisotropic grain shape of plagioclase in most layered gabbroic rocks, the poles to (010) are commonly subperpendicular to the compositional layering (e.g. paleo-vertical within a melt lens or magma chamber), even in "quasi-static" layered intrusions. For lower oceanic crust formed via the Gabbro Glacier mechanism, the upper gabbros would be expected to have plagioclase fabrics showing (010) maxima parallel to the spreading direction, with a vertical maximum in [100], owing to the dominantly vertical flow field. With increasing depth, the plagioclase (010) poles would be expected to rotate with the orientation of the compositional layering, such that at the base of the crust the lower gabbros will have a vertical alignment of (010) and a strong horizontal alignment of [100] sub-parallel to the spreading direction. In contrast, for the Sheeted Sills mechanism, all gabbros regardless of their depth within the crustal section should show alignment in the plagioclase (010) poles parallel to the paleo-vertical (e.g. the direction of the sheeted dikes), with no strong lineation demonstrated by the [100] axis.

3. Methods

Here we present plagioclase fabrics from gabbros throughout the lower crustal stratigraphy to compare with the different predictions of strain in the Gabbro Glacier vs. Sheeted Sills hypotheses for fast spreading ridges.

The geochemistry of lavas in the Samail ophiolite is systematically different from that of lavas from mid-ocean ridges (e.g., Pearce et al., 1981; MacLeod et al., 2013). Gabbroic rocks also differ; evolved Oman gabbros rarely contain abundant orthopyroxene, and commonly contain igneous hornblende (e.g., Pallister and Hopson, 1981), unlike evolved mid-ocean ridge gabbros (e.g., Mevel et al., 1996). Nevertheless, crustal thickness and layering are similar to that inferred for fast- to intermediate-spreading mid-ocean ridges from seismic data (e.g., Vera et al., 1990). In the absence of evidence to the contrary, we infer that the mechanism of igneous crustal accretion in the Samail ophiolite was similar to that at fast- to intermediate-spreading mid-ocean ridges such as EPR or Juan de Fuca.

Samples were collected through a 4700 m stratigraphic section of lower crustal gabbros in the Wadi Tayin massif of the Samail ophiolite (Fig. 3, Supplementary Table 1). This sample section corresponds approximately to the Khafifah section, mapped and sampled by Pallister and co-workers (Pallister and Hopson, 1981). 13 oriented samples were cut perpendicular to the foliation (defined by the visible modal layering, typically corresponding to the plagioclase shape preferred orientation in hand specimen) and parallel to the lineation (where identifiable). Near the top of the section, in the isotropic or varitextured gabbros, modal layering is not well-defined and the foliation is defined by alignment of tabular plagioclase crystals. Polished thin sections were then further polished using colloidal silica for electron backscatter diffraction (EBSD) analyses. Crystallographic orientations (LPOs) were measured at the Marine Biological Laboratory/Woods Hole Oceanographic Institution on a JEOL 840 SEM at 20 kV with a beam current of 60 nA, and at Brown University on a JEOL 845 SEM at the same operating conditions. For each individual thin section, between 250 and 500 individual plagioclase grains were manually analyzed and their orientations determined using the HKL Channel 5+ software after visual inspection of diffraction patterns.

In the layered gabbros the foliation is defined as being parallel to the modal and compositional layering in the rock. Near the top of the section, in the isotropic or varitextured gabbros, modal layering is not well-defined and the foliation is defined by alignment of tabular plagioclase crystals. Pole figures for each sample were rotated into a geographic reference frame, to facilitate comparison with the crustal accretion models. The average strike of the sheeted dikes in this region is 341° (Nicolas et al., 1988a; Fig. 3). Rotations into the geographic reference frame (with the paleo-vertical orientated N or 0°) also account for the regional strike and dip of the paleo-horizontal based on the orientation of the crust-mantle boundary and the sheeted dike/gabbro boundary (Fig. 3). All fabrics are rotated such that the primitive of the pole figures is 071/55, which is a paleo-vertical plane perpendicular to the sheeted dikes (see thick red line in Fig. 3). In Wadi Khafifah, the mean orientations of the sheeted dikes and Moho are not perpendicular, but are at an angle of approximately 60–70° to one another. Thus, in our geographic reference frame, the pole to the sheeted dikes has an azimuth of 270, and the pole to the layering of samples with layer orientations parallel to the Moho ends up ∼20–30° away from the paleo-spreading direction inferred from the dikes. The 20–30° discrepancy is consistent with the location of an emplacement related fold (The Ibra Valley Syncline; Pallister and Hopson, 1981) that is mapped in our study area (Fig. 3).

Fabric strength is quantified using the M-index procedure of Skemer et al. (2005) and the J-index, C-factor, and K-factor are calculated for each sample from the software of D. Mainprice (http://www.gm.univ-montp2.fr/mainprice//CareWare_Unicef_Programs).

4. Results

From the well-defined plagioclase LPOs (Fig. 4), and the lack of any other strong plastic deformation indicators, such as subgrains, undulatory extinction or grain size reduction by dynamic recrystallization, we infer that the plagioclase LPOs measured here are magmatic and have not experienced any significant amount of submagmatic or subsolidus deformation (e.g. Nicolas et al., 1988a).

Pole figures for the rotated plagioclase fabrics reveal two groups of samples divided on the basis of their mean orientations. The uppermost samples, hereafter referred to as the "upper gabbros", have plagioclase fabrics with [100] steeply rotated near-vertical with respect to the paleo-seafloor (Fig. 4). The upper gabbros include samples OM97-113, OM97-204, OM97-111. The deepest of these, OM97-111, is located at 3594 m above the Moho, corresponding to ∼1100 m stratigraphically below the sheeted dikes in this region. One sample, OM97-106, located at 3260 m above the Moho, appears to be transitional between the upper gabbros and those below. All samples stratigraphically below this point, hereafter referred to as the "lower gabbros", have plagioclase [100] aligned sub-parallel to the Moho in this region (Fig. 4). We use the terms upper and lower gabbros here in place of the commonly used terms "foliated gabbros" and "layered gabbros", as these terms have come to mean different things to different authors based on petrofabrics as well as geochemistry.

The steeply oriented plagioclase fabrics of the upper gabbros in the geographic reference frame is unsurprising given the same observation of near-vertical orientation of modal and compositional layering made at the outcrop-scale previously recognized by numerous workers (Pallister and Hopson, 1981; Smewing, 1981; Henstock et al., 1993; Quick and Denlinger, 1993; Nicolas et al., 1988a; Phipps Morgan and Chen, 1993; Boudier et al., 1996; MacLeod and Yaouancq, 2000). However, aside from the change in mean orientation observed at the outcrop-scale, there does not appear to be any other difference in plagioclase fabrics between the upper and lower gabbros. Additionally, there is no change in the whole rock geochemistry or modal assemblage that would distinguish the majority of the upper gabbros from the lower gabbros. Only sample OM97-113 has the characteristic high incompatible trace element contents and magmatic amphibole that is typically associated with the 'isotropic' gabbros (e.g. Kelemen et al., 1997).

The Gabbro Glacier model predicts that shear strain in the gabbros will increase with depth in the crust (Fig. 2). Increasing shear strain, and the change in flow lines with depth, will result in three main features in the plagioclase fabrics, applicable at both the crustal-scale and the individual sample level: (1) progressive alignment of the a-axis maxima, such that [100] orientations form a point maximum and not a girdle; (2) increasing fabric strength in all axes; (3) rotation of the fabric with depth to become parallel to the crust-mantle boundary. A fourth feature, the obliquity of the plagioclase LPO with respect to the compositional layering, can be used to assess the degree of shear strain, with the caveat that experiments and models show that pure shear and simple shear can produce similar fabrics under some conditions.

4.1. Plagioclase LPO: Alignment of [100]

While all samples have well-defined (010) maxima, only a subset of samples have distinctive maxima in [100], and no samples cross the girdle-cluster transition defined by the K-factor (Fig. 6). The development of a cluster or point maximum in [100], e.g. a lineation, is typically associated with a dominant magmatic flow direction or increased shear strain (e.g. Ildefonse et al., 1992a, 1992b).

On the crustal scale, the lower gabbros have point-maxima in poles to (010) that are oriented perpendicular to the Moho (Fig. 5), whereas the uppermost gabbros have point-maxima in poles to (010) aligned near the paleo-horizontal. However, there is no geographic preferred orientation of the [100] maxima with depth below the paleo-AMC (Fig. 5; Supplementary Table 2). The lack of a systematic orientation direction of the [100] maxima indicates heterogeneous deformation kinematics during fabric formation and thus is inconsistent with systematic alignment due to shear strain, as predicted in the Gabbro Glacier hypothesis. High degrees of either pure or simple shear can result in the alignment of plagioclase [100] axes, causing a transition from girdle to point maxima in [100] and an increase in fabric strength, as quantified by the K-factor and the C-factor, respectively (Fig. 6). All samples measured here have low [100] K-factors – below the girdle/cluster transition defined by Woodcock (1977) – and there is no systematic change in these parameters with depth in the lower crustal section (Fig. 6).

4.2. Plagioclase LPO: fabric strength

In addition to the lack of systematic variation in the orientation and strength of [100] maxima with depth, there is no correlation between fabric strength in any crystallographic axis with its

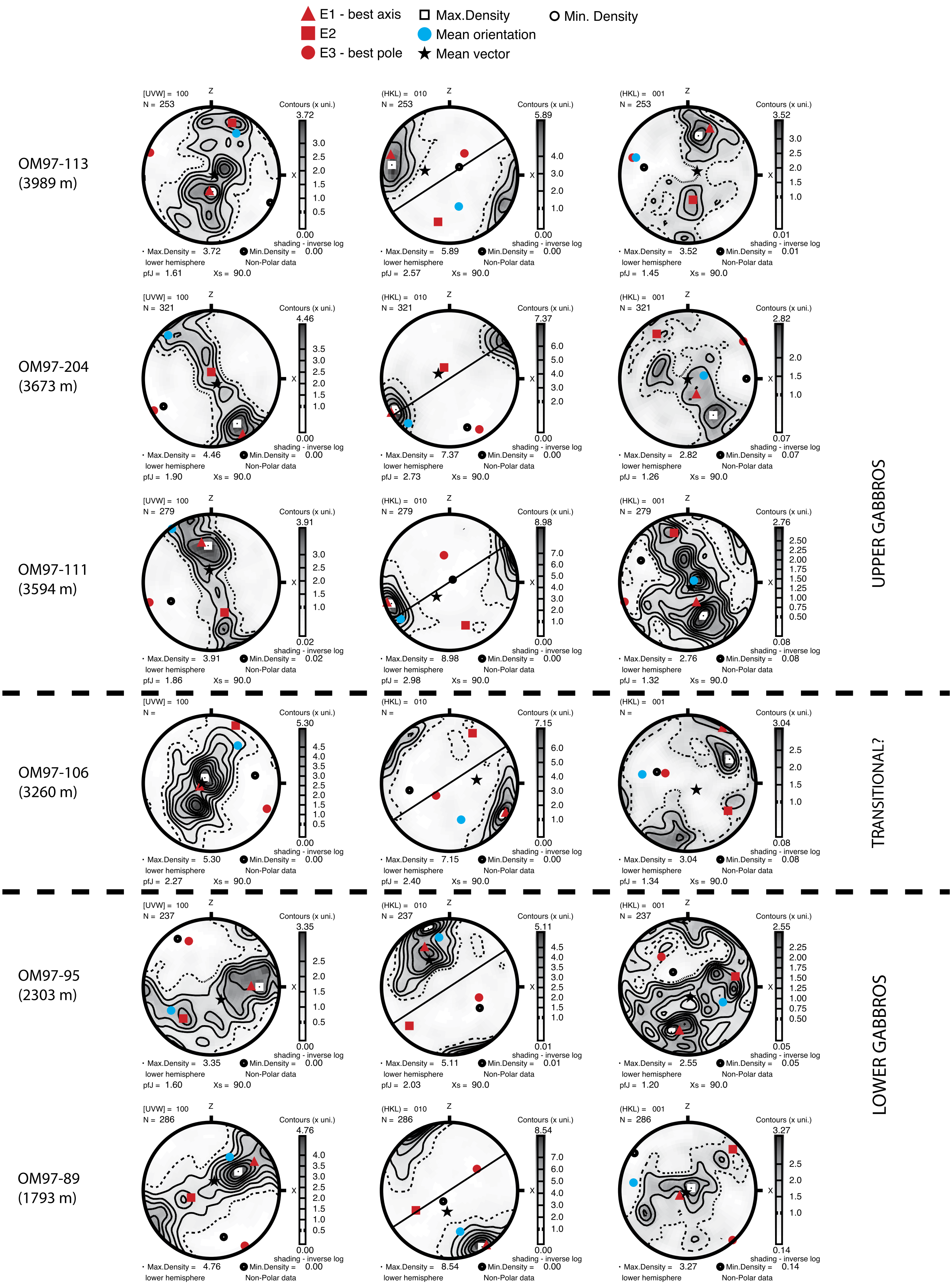
E1 - best axis
E2
E3 - best pole
Max.Density
Mean orientation
Mean vector
Min. Density
OM97-113
(3989 m)
OM97-204
(3673 m)
OM97-111
(3594 m)
OM97-106
(3260 m)
OM97-95
(2303 m)
OM97-89
(1793 m)
UPPER GABBROS
TRANSITIONAL?
LOWER GABBROS
[UVW] = 100
(HKL) = 010
(HKL) = 001
Contours (x uni.)
shading - inverse log
lower hemisphere
Non-Polar data

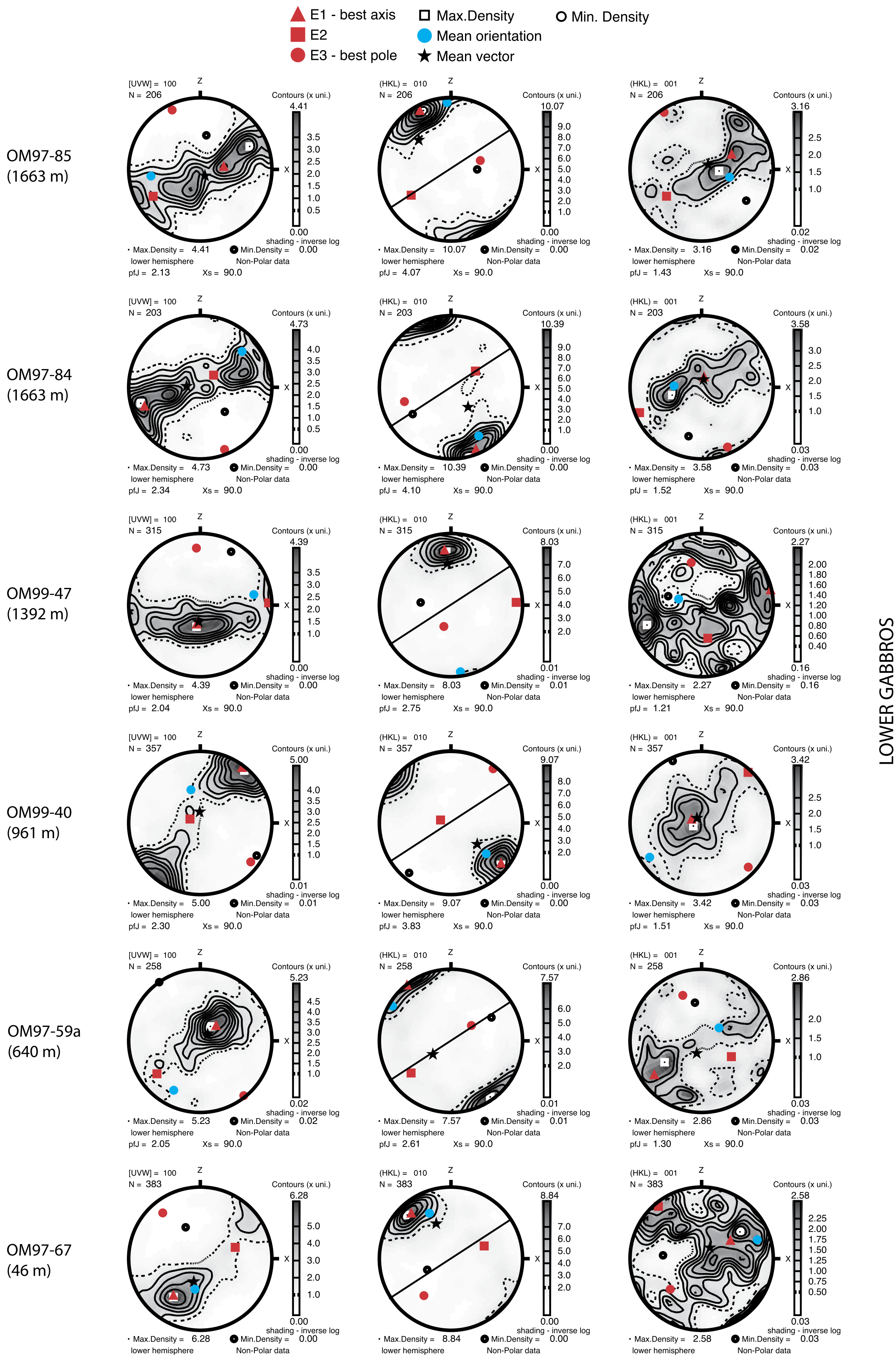

Fig. 4. (*continued*)

Fig. 4. Plagioclase pole figures rotated into the geographic reference frame. Pole figures were generated using the software of D. Mainprice (ftp://www.gm.univ-montp2.fr/mainprice//CareWare_Unicef_Programs/). Samples are arranged according to stratigraphic height. The base of the crust, the Moho, corresponds to a height of 0 m. Symbols corresponding to the best axis, best pole, maximum density, mean orientation, mean vector, and minimum density are generated automatically using the statistics option in the Mainprice software. Symbol legend is at the top center of the figure. All orientations and statistics are provided in the Supplementary Material. Note: the 20–30° obliquity of the (010) maxima with respect to the vertical in the lower gabbros is an artifact of the geographic reference frame chosen. The sheeted dikes and Moho are not perpendicular to one another in the Wadi Khafifah crustal section, but are 60–70° oblique to one another. The Moho plane in the geographic reference frame is provided for visual reference as a dark black line in the (010) pole figures for each sample.

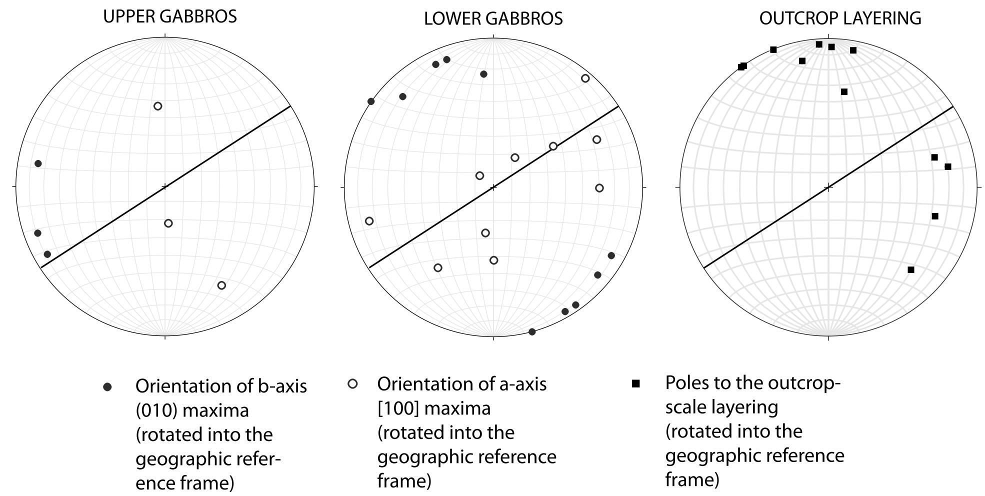

Fig. 5. Orientation of [100] maxima (open circles) and (010) maxima (filled circles) from pole figures shown in Fig. 4. In the geographic reference frame, an inclination of 0° corresponds to the paleo-vertical. (a) In the upper gabbros, the (010) maxima are aligned nearly perpendicular to the sheeted dikes, and there is no preferred orientation direction in the [100] maxima. (b) In the lower gabbros, (010) maxima are aligned perpendicular to the Moho (60–70° oblique to the sheeted dikes), and [100] maxima show no clear preferred orientation. (c) Orientation of the pole to the outcrop-scale compositional layering, rotated into the geographic reference frame (55/071). These results suggest that there is no preferred strain orientation or development of a dominant lineation direction on the crustal scale, which would result in alignment of a-axis maxima into a single direction. Rather, the data are more consistent with magmatic compaction throughout the lower crust.

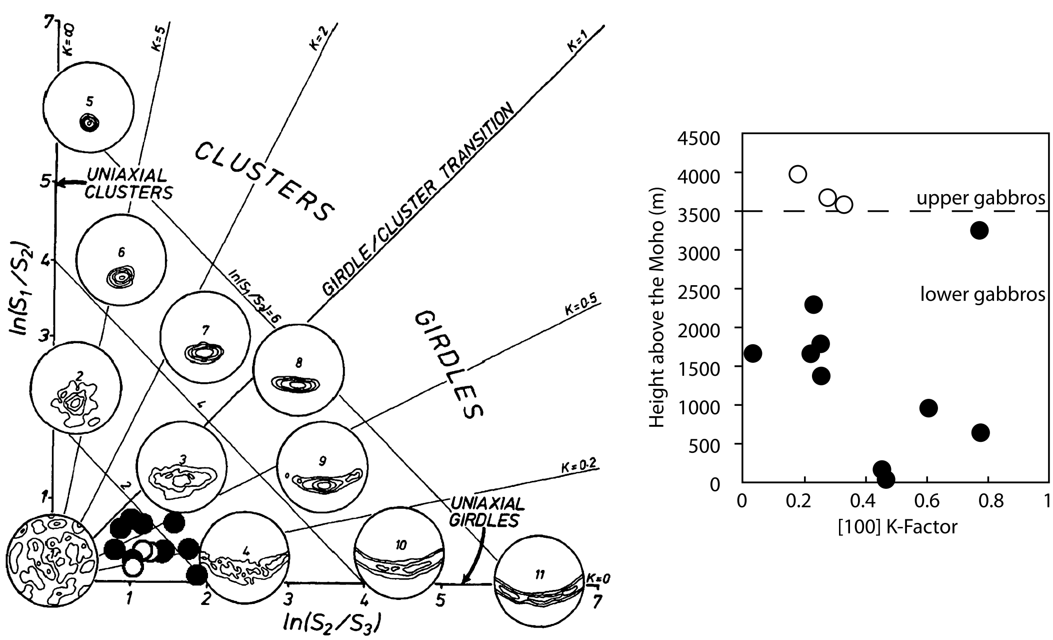

Fig. 6. (a) C-factor and K-factor measured for the [100] axis indicating that the plagioclase samples measured here are dominated by girdles in the [100] axis. Base figure is taken from Woodcock (1977) for illustration. (b) [100] K-factor with height above the Moho. There is no systematic change in K-factor with stratigraphic height as would be expected during increasing crystal alignment due to shear strain in the Gabbro Glacier mechanism.

stratigraphic height above the Moho, and there is no difference in plagioclase fabric strength between the upper and lower gabbros. The pfJ-index quantifies the fabric strength for each individual axis, with higher values indicating a stronger or more aligned fabric. In the case of all samples measured here, no systematic increase in pfJ-index for any axis is observed (Fig. 7; Suppl. Table 2), and no change in the overall J-index of the sample (Fig. 7; Suppl. Table 1).

The M-index (Skemer et al., 2005) can also be used to quantify the fabric strength of the rock and is less dependent on the number of grains analyzed. The M-index varies from 0, where the fabric is completely random, to 1, where the fabric is completely aligned. All samples measured here have M-indices between 0.07–0.19, and no trend is observed with increasing depth (Supplementary Table 1, Fig. 7).

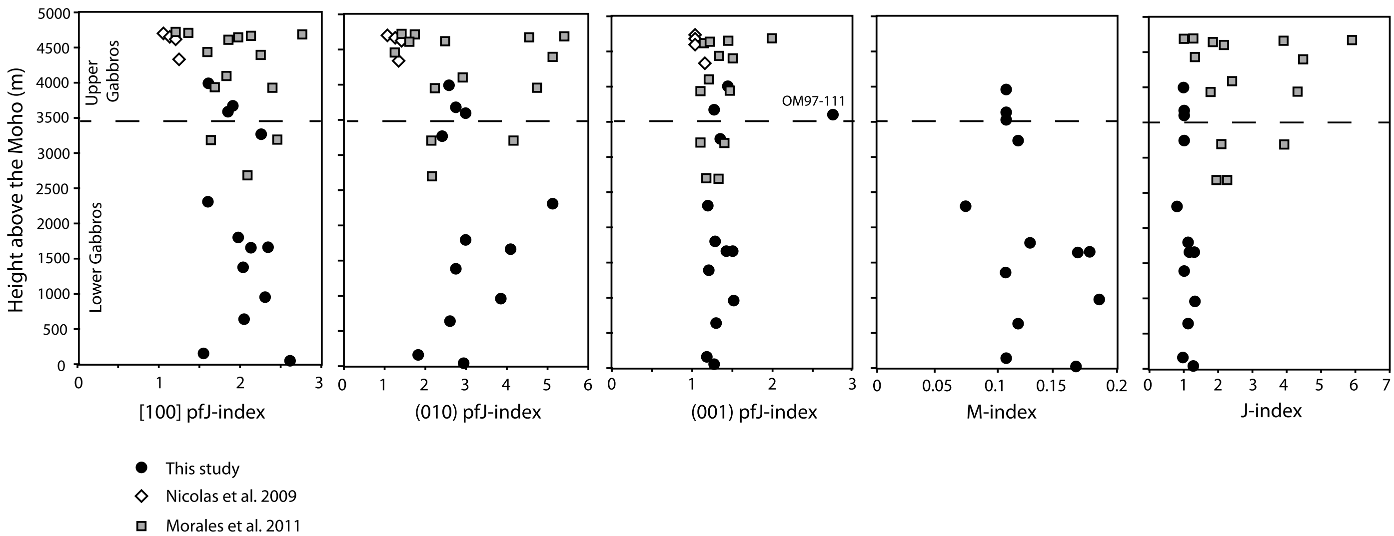

Fig. 7. Fabric strength with depth as quantified by the J-index for each individual axis and the overall J-index and M-index of each sample (black circles). All fabric strength, orientation, and statistical data can be found in Supplementary Tables 1 and 2. There is no trend in any measure of the fabric strength with depth in the crustal section analyzed here. White triangles are data from Nicolas et al. (2009), and gray squares are anorthosite samples from Morales et al. (2011). Stratigraphic height for the data of Nicolas et al. (2009) and Morales et al. (2011) were reported in meters relative to the sheeted dikes. The sheeted dikes in the Wadi Khafifah region are located at ∼4700 m.

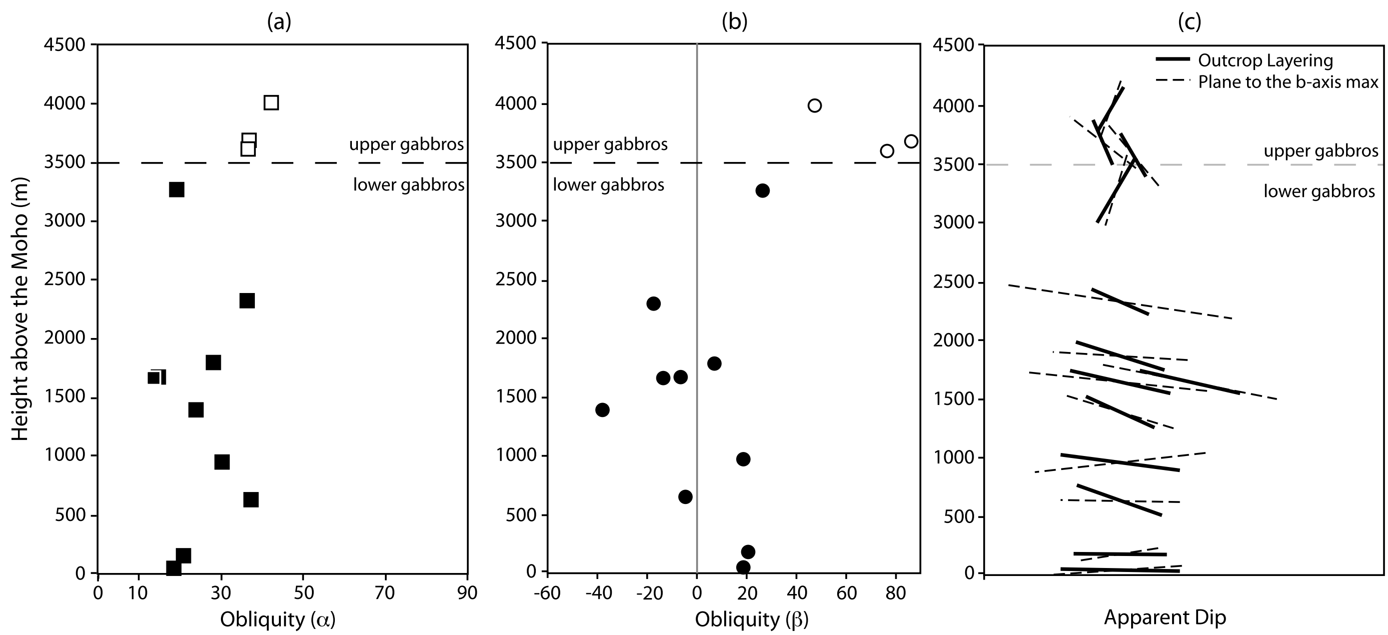

Fig. 8. (a) Obliquity, α, between the (010) maxima and the pole to the compositional layering measured in outcrop. There is no trend of decreasing obliquity with depth, as would be predicted by the Gabbro Glacier hypothesis. (b) Obliquity, β, measured between the (010) maxima and the pole to the Moho rotated into the geographic reference frame. (c) Reconstructed apparent dips of the outcrop layering (thick solid line) and the plane to the b-axis maxima (thin dashed line) after rotation into the geographic reference frame; Top = 0°; East = 90°. Line lengths are proportional to the fabric strength, such that the length of the outcrop layering is proportional to the overall J-index of the sample and the length of the b-axis maxima plane is proportional to the (010) pfJ-index. Due to the location of the Ibra Syncline near the top of the Khafifah section, the layering in gabbros near the Moho dip of 35°N, whereas the Sheeted Dikes in this region are approximately vertical (Fig. 3; and Fig. 2c of Pallister and Hopson, 1981; also see Nicolas et al., 1988a). Thus, samples collected to the NW of the red orientation line in Fig. 3 (e.g. all of the lower gabbros with the exception of OM97-106) were rotated 35° clockwise, whereas samples collected to the SE of the line (e.g. the upper gabbros and OM97-106) were not rotated. There is a consistent top to the right shear sense between the b-axis plane and the outcrop scale layering. The angle of obliquity between the b-axis plane and the layering is approximately constant (20–40°) implying low shear strains throughout the lower crust.

4.3. Plagioclase LPO: obliquity

As noted above, obliquity of fabrics during shear depends on the aspect ratio of the grains and the relative contributions of simple and pure shear (e.g., Ghosh and Ramberg, 1976; Ildefonse et al., 1992a, 1992b). During torsional experiments on magmatic suspensions of plagioclase, Picard et al. (2011) showed that plagioclase within a thin shear zone aligns such that [100] is subparallel to the macroscopic shear direction, whereas plagioclase outside the shear zone aligns with [100] approximately 45° relative to the shear direction. The narrow shear zone is oriented ∼20° clockwise from the macroscopic dextral shear direction – thus the [100] axes remain oblique to the local kinematic reference, nominally consistent with previous experimental and modeling work. Furthermore, comparisons of these studies indicate that the conditions where "steady state" fabrics are produced are not well defined. In any case, it is difficult to distinguish between pure shear and simple shear on the basis of plagioclase obliquity alone.

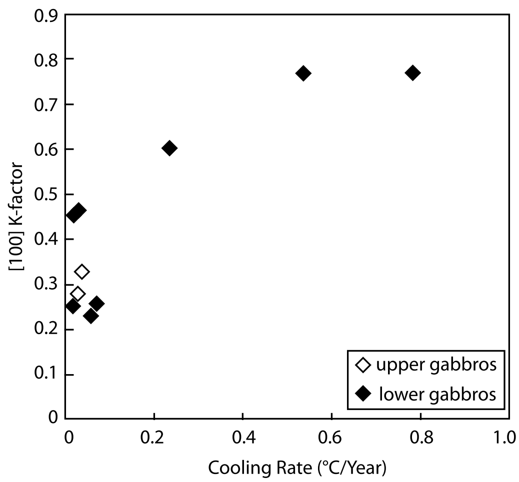

Fig. 9. Correlation of cooling rates with plagioclase [100] K-factor. Cooling rate of each sample through the ∼750–800 °C isotherm is measured by Ca diffusion in olivine; data from VanTongeren et al. (2008). Samples with very fast cooling rates were previously inferred to have intruded off-axis. The three samples (OM97-59a, OM99-40, and OM97-106) with very fast cooling rates are also the three samples with high [100] K-factor (e.g. stronger lineation). It is possible that the off-axis sills experienced a different strain history during crystallization; however, there is no correlation between cooling rate and any other plagioclase LPO metric. More work must be done to confirm, quantify and understand this relationship.

The obliquity we measured between the (010) maxima and the outcrop scale layering (α) does not vary systematically with depth over the crustal section, nor does the obliquity between the (010) maxima and the pole to the Moho (β) (Fig. 8). Owing to the number of variables that control the evolution of fabric obliquity with strain, it is difficult to quantify the strain magnitude in our samples. However, because the obliquity between the layers and the (010) fabric remains ∼20° to 40° (Fig. 8) our observations indicate that shear strain does not vary significantly with depth. Furthermore, the (010) maxima are always oriented counterclockwise from the pole to layering in the geographic reference frame (Fig. 8c), indicating a constant sense of shear with depth. At face value, these observations are inconsistent with the Gabbro Glacier model because the steep orientations of the strain ellipses in the Glacier model for more shallow portions of the crust (i.e. Fig. 2) are formed by dominantly vertical flow with a shear sense opposite that imposed by the dominantly horizontal flow deeper in the crust. In addition, while more equivocal, the ∼20° to 40^{o} obliquity suggests shear strains on order of 1 or less assuming simple shear (e.g., Picard et al., 2011), or even lower if deformation involves a significant component of pure shear (cf. Ghosh and Ramberg, 1976) or compaction.

4.4. Off-axis vs. on-axis emplacement: correlation with cooling rates

VanTongeren et al. (2008) noted that there was no systematic trend in the cooling rate of samples with depth in the Wadi Khafifah stratigraphy. In order to explain inferred cooling rates through the 800° isotherm of ∼1 °C/yr that are faster than predicted in models of hydrothermal convection, they suggested that some samples may have been emplaced as off-axis sills, where host-rock temperatures were markedly colder. This interpretation is consistent with recent seismic imaging of mid-crustal melt bodies several kilometers off-axis at both Juan de Fuca ridge (Canales et al., 2009) and the East Pacific Rise (Canales et al., 2012).

Samples OM97-59, OM97-106, OM99-40 record cooling rates that are an order of magnitude faster than most of the others (Supplementary Table 1). The cooling rate measured for each sample is uncorrelated to most metrics of plagioclase fabric strength, though all three samples that cooled very rapidly also show the highest K-factor (or point-maxima) in the [100] axis (Fig. 9). While difficult to quantify from this observation alone, it is possible that sills intruded off-axis are subject to a significantly different deformation history during crystallization than those formed on-axis.

4.5. Difference between gabbroic fabrics and anorthositic fabrics?

In nearly all metrics analyzed, there is no statistical difference in the shape, strength, or obliquity of the plagioclase LPO recorded between a gabbroic sample (OM97-85; 50–60 volume % plagioclase) and an anorthosite layer (OM97-84; >90 volume % plagioclase) located within the lower gabbros at 1663 m above the Moho (Fig. 4, Supplementary Table 2). The nearly identical LPO in these two samples suggests that rocks emplaced at the same stratigraphic level will generally experience the same deformation history. Future work ‘mapping’ the LPO of closely spaced samples from a small stratigraphic section may provide a record of individual sill emplacement within the crust.

There is no difference in the fabric strength in any crystallographic axis, as quantified by the pfJ-index, in the anorthosite samples of Morales et al. (2011) compared to those of the gabbro samples reported in this study (Fig. 7). At face value, this observation suggests that formation of anorthosite layers in the lower oceanic crust is not due to increased shear strain (e.g. Jousselin et al., 2012) or input of new magma (e.g. Boudier and Nicolas, 2011) as previously hypothesized, but that they likely form as a result of typical magma chamber processes, similar to the processes that form anorthositic layers in undeformed, continental layered intrusions.

5. Discussion

5.1. Comparison with fabrics from other levels in the Samail ophiolite

5.1.1. Comparison to observations at the Root Zone of the Sheeted Dike Complex (RZSDC), Samail Ophiolite

Very few systematic studies of plagioclase fabrics in the gabbroic lower crust have been reported to-date. A study of plagioclase fabrics in gabbros from the Wadi Al Abyad section of the Nakhl Rustaq block of the Samail ophiolite (Yaouancq and MacLeod, 2000) was undertaken to quantify whether magnetic anisotropy was related to plagioclase LPO in the oceanic crust. This study included seven samples predominantly from the uppermost oceanic crustal section, with only two samples from layered gabbros lower in the section. Both lower gabbro samples showed well-defined maxima in (010). A strong lineation (maxima in [100]) was found in one sample. The lower gabbro LPOs were not significantly different from those reported for samples higher in the crustal section.

Nicolas et al. (2009) documented a series of plagioclase fabrics in gabbros inferred to have formed within or very near to the paleo-AMC in the Samail ophiolite. They concluded that the steep magmatic foliations seen in some rocks within 10s of meters of the RZSDC were formed due to subsidence along the magma chamber walls prior to moving horizontally away from the AMC. They showed plagioclase pole figures for five samples from 0 m below the RZSDC to 365 m below. Two samples, found at 45 m below the RZSDC and 80 m below, appear similar to the upper gabbro samples OM97-204 and OM97-111, though they have a slightly lower [100] J-index than those measured here (Fig. 7). The other samples measured by Nicolas et al. (2009) lack a strongly defined LPO.

Morales et al. (2011) examined anorthosite layers from the same regions as Nicolas et al. (2009), and divided their samples into three categories: upper anorthosites with flat-lying foliation, upper anorthosites with steep foliations, and anorthosites found within the lower gabbros near the Moho. Of the four anorthosites measured by Morales et al. (2011) from the lower gabbro section, all samples have point maxima in (010), and girdles in [100], and the fabric strength in both [100] and (010) overlaps with that observed in the gabbros measured throughout the lower crust in our study (Fig. 7).

5.1.2. Comparison to the Mantle Transition Zone gabbros in the Samail ophiolite

In their study of gabbro lenses within dunite and residual mantle peridotite in the Moho Transition Zone (MTZ), Jousselin et al. (2012) noted that some lenses display nearly isotropic plagioclase fabrics (their Type 1 sills), others show pronounced magmatic fabrics and modal layering (their Type 4 sills), while two other groups (Types 2 and 3 sills) are intermediate between these end-members. They conclude that the layering and plagioclase fabrics in the lenses are the result of increasing simple shear during magmatic deformation due to mechanical coupling with the surrounding mantle flow, and suggest that layering is formed by rotation of the particles into the shear plane and segregation from one another based on size and density sorting.

The plagioclase fabrics seen in the MTZ Types 2–3 lenses of Jousselin et al. (2012) are qualitatively indistinguishable from those seen throughout the lower crustal gabbros shown here, though no J-indices are provided for quantitative comparison. Sample OM97-45, located *ca*. 162 m above the Moho, has a nearly identical fabric to their Type 2 sills; whereas sample OM97-67, located *ca*. 46 m above the Moho, has a fabric similar to their Type 3 sills. Other samples that have similar fabrics to Types 2 and 3 lenses occur at all levels in the crustal section we analyzed and in some cases are near those with poorly-defined lineations in [100]. For example, sample OM97-85 occurs only ∼100 m stratigraphically below sample OM97-89 in the middle of the section, yet has a much stronger maximum in [100].

If the interpretation of Jousselin et al. (2012), that mechanical coupling with mantle flow is the dominant control on igneous layering and plagioclase LPO, were applied to the entire lower crust, then one would expect a gradual decrease in deformation strength from the base of the section to the top – similar to the prediction based on the Gabbro Glacier hypothesis (Fig. 2). Instead, there is no systematic variation in plagioclase LPOs with depth in the section we have studied.

5.2. Plagioclase fabrics in the lower crust

Our data reveal five important criteria that should be met in evaluating models for the formation and accretion of the lower oceanic crust:

(1) There is a distinctive change in the orientation of the outcrop-scale layering from near-vertical to sub-horizontal that is also reflected in the plagioclase fabrics in the uppermost ∼1000–1500 m of the gabbroic crust (Pallister and Hopson, 1981; Smewing, 1981; Henstock et al., 1993; Quick and Denlinger, 1993; Nicolas et al., 1988b; Phipps Morgan and Chen, 1993; Boudier et al., 1996; MacLeod and Yaouancq, 2000; Figs. 3, 5).

(2) The distinction between the upper gabbros and lower gabbros is not a geochemical boundary. The change in outcrop-scale orientation from near-vertical to sub-horizontal occurs stratigraphically lower in the crust than a change in whole-rock geochemistry (e.g. Kelemen et al., 1997). Only the uppermost sample, OM97-113, lacks clear compositional layering or foliation. It also contains amphibole and has significantly higher whole-rock REE contents than the rest of the stratigraphy. OM97-113 is located 3989 m above the Moho and is representative of the so-called isotropic or varitextured gabbros observed throughout the top of the crustal section in the Oman ophiolite (e.g. MacLeod and Yaouancq, 2000). However, the other upper gabbro samples, OM97-111 and OM97-204 possess distinctive compositional layering, and have similar whole rock REE contents and modal abundances to the lower gabbros, they also have no amphibole or magnetite in their phase assemblage.

(3) There is no systematic difference in plagioclase fabric strength in any crystallographic axis between the upper gabbros and the lower gabbros (Fig. 7).

(4) Beneath the abrupt transition from sub-vertical to sub-horizontal fabric, there is no systematic change in the geographic orientation of the plagioclase fabric, or in the development of a dominant lineation direction within the upper gabbros or the lower gabbros (Fig. 5).

(5) In the lower gabbros, the obliquity between the (010) and the modal layering remains approximately constant and indicates a consistent sense of shear with depth (Fig. 8). By removing the rotation of layers caused by the emplacement-related Ibra Valley Syncline (Fig. 8c), the layers become more sub-parallel to the crust-mantle boundary throughout the lower gabbro section.

Together, these 5 criteria are inconsistent with predictions of the changing kinematics, increasing fabric strength or increasing shear strain from the sheeted dikes to the Moho that are required by the Gabbro Glacier hypothesis. In the lower gabbros, the maximum principle stress direction was vertical (e.g. perpendicular to the Moho), as indicated by the compaction-dominated plagioclase fabrics shown in Fig. 4 and the lack of preferential alignment in the [100] axes (Fig. 5). These observations suggest that the majority of the gabbroic crust of the Samail ophiolite was crystallized *in situ* in small melt lenses, as proposed in the Sheeted Sill hypothesis. The upper gabbros also have a lack of preferential alignment in the [100] axes and show no difference in the strength of the plagioclase fabric compared with the lower gabbros. However, the steep near-vertical orientation of the compositional layering and plagioclase fabrics in the upper gabbros is difficult to reconcile with either the Gabbro Glacier or Sheeted Sills model for oceanic lower crust formation.

Boudier et al. (1996, Fig. 7) proposed a hybrid model in which the lower "layered" gabbros were formed by multiple sill injections into a gabbro glacier, and the upper "foliated" gabbros were formed in the AMC and gained their final orientations in the Gabbro Glacier (also see Korenaga and Kelemen, 1998, Fig. 9c). Similarly, even in their figure illustrating an "end-member" Sheeted Sill model, Kelemen et al. (1997, Fig. 6) included a small Gabbro Glacier overlying a lower crustal section formed from sheeted sills, as did Korenaga and Kelemen (1998, Fig. 9d) and Maclennan et al. (2004, Figs. 1 and 12). While these hybrid models are consistent with the steep orientations of the upper gabbros (observation #1), they are unable to explain the lack of [100] alignment in our upper gabbro samples (observation #4) or the similarity of fabric strength between the upper and lower gabbros revealed in our dataset (observation #3). For example, if the upper gabbros were accreted in a Gabbro Glacier setting, the plagioclase fabrics should show the development of a preferred lineation with stratigraphic depth, and should possess a stronger fabric than those accreted in a compaction-only setting like the lower gabbros. These trends are not observed. However, there is a gap in our sampling over the potentially critical interval between the upper and lower gabbros, and we have analyzed only three samples representing the upper gabbros. More detailed sampling over the uppermost 1–1.5 km below the sheeted dikes may distinguish between the various hybrid models discussed above.

The observations of plagioclase fabrics in crustal gabbros of the Oman ophiolite are most consistent with the model proposed by MacLeod and Yaouancq (2000) in which the steep foliations observed in the upper gabbros are formed in a magma mush column that is responding to interstitial melt migration from the lower gabbros into an axial magma chamber. In their model, MacLeod and Yaouancq (2000) suggest that the upper gabbros "do not... represent transposed cumulus layers but reflect the trajectory of flow of the crystal mush as the melt fraction decreases through the 'rigidus'... at ∼20–40% melt fraction." The model of MacLeod and Yaouancq (2000) explains the abrupt transition in the gabbros from flat-lying to near-vertical without any other significant changes in the character of the plagioclase fabrics or geochemistry.

In Wadi Abyad, where MacLeod and Yaouancq (2000) first proposed their model, the transition from horizontally layered lower gabbros to steeply foliated upper gabbros occurs at ∼1700 m stratigraphically above the Moho in a ∼2600 m thick lower crust. In Wadi Tayin, where our study is focused, this transition occurs at ∼3260 m (sample OM97-106) in a ∼4700 m thick lower crust. Thus, the fraction of the plutonic lower oceanic crust formed as layered gabbro (∼60–70%) in these two sections is independent of the total crustal thickness. The consistent ratio of lower gabbros to upper gabbros suggests that the transition from flat-lying to steep foliations is not due to vertical flow and lateral movement away from the ridge axis as hypothesized in the Gabbro Glacier or Hybrid models. These models would predict a gradual transition from steep to flat-lying foliations at a constant depth independent of crustal thickness.

5.3. Comparison with slow and ultra-slow spreading ridges

Our results suggest that the majority of extensional deformation in fast-spreading ridges is localized at the ridge axis due to the presence of small melt lenses distributed throughout the crust. This hypothesis is consistent with seismic compliance results, which estimate between 5 and 25% melt present throughout the lower crust of the EPR (e.g., Zha et al., 2014); and with the clear presence of several distinctive sub-axial melt lenses distributed throughout the lower crust along the EPR (Marjanović et al., 2014).

In contrast to fast spreading ridges, at slow and ultra-slow spreading centers melt supply is limited. Mehl and Hirth (2008) analyzed plagioclase LPOs in several gabbro mylonites found in narrow (∼0.2 mm) shear zones throughout the 1.5 km section of gabbroic ocean crust recovered in ODP Hole 735B from the ultra-slow spreading Southwest Indian Ridge (SWIR). Inside the shear zones, in polyphase bands, grain size was significantly reduced, grains were recrystallized and the LPO was destroyed. In plagioclase-rich bands, on the other hand, grain sizes were larger, there was evidence for crystal plastic deformation, and plagioclase LPOs had strong maxima in [100] perpendicular to maxima in poles to (010). In samples from between the shear zones, Mehl and Hirth (2008) documented the presence of an LPO formed prior to strain localization. All of the plagioclase [100] axes in these samples are aligned parallel with the shear plane and show distinct maxima in the pole figures. These fabrics are illustrative of localized, plastic deformation of gabbroic crust at ultra-slow spreading ridges, where melt supply to the ridge axis is extremely limited.

A recent study of the Kane oceanic core complex along the slow-spreading Mid-Atlantic Ridge (Hansen et al., 2013) found plagioclase fabrics similar to those documented for the ultra-slow SWIR (Mehl and Hirth, 2008). Lower crust and upper mantle lithologies along the Kane detachment fault were extensively mylonitized, with high temperature (>700 °C) deformation leading to extreme crystal-plastic deformation and near destruction of the plagioclase LPO. Samples with the strongest LPO displayed alignment of the plagioclase [100] axes aligned with the shear direction, and poles to (010) perpendicular to the shear plane.

There are very few ductile shear zones identified in the crustal section of the Samail ophiolite, and no known evidence of detachment faulting. The lack of significant submagmatic and subsolidus plastic deformation recorded in the gabbro cumulates suggests that the extensional stress associated with rifting at mid-ocean ridges is accommodated differently in the lower crust at fast versus slow spreading ridges.

6. Conclusions

Plagioclase LPOs measured throughout the lower crust of the Samail ophiolite show no systematic change in shape, strength, or obliquity with depth (Figs. 4, 6, 7, 8). In the lower gabbros, poles to plagioclase (010) are aligned paleo-vertical and have maxima perpendicular to the inferred paleo-spreading direction (Fig. 5). In the upper gabbros, the plagioclase LPO reflects the mean outcrop-scale layering and is steeply oriented, with foliation and layering nearly parallel to the sheeted dikes. Plagioclase [100] maxima show no preferred direction of alignment within the crust, indicating no systematic orientation of shear strain (Fig. 5), and [100] fabrics approach but do not cross the girdle-cluster transition defined by the K-factor, and thus lack a strong lineation (Fig. 6).

We list five observations that must be satisfied by any crustal accretion model. Our observations are inconsistent with Gabbro Glacier and Hybrid models involving a crustal-scale glacier. Instead, our results are most consistent with the Sheeted Sills hypothesis, and suggest that rotation of the outcrop-scale layering from sub-horizontal in the lower gabbros to sub-vertical in the upper gabbros is due to preferential alignment during vertical interstitial melt flow to the axial magma chamber as proposed by Macleoad and Yaouancq (2000). The Samail ophiolite formed at a fast-spreading submarine spreading center, and our results suggest that the majority of extensional deformation in fast-spreading ridges is localized at the ridge axis by the presence of small melt lenses distributed throughout the crust.

Acknowledgements

J.V.T. acknowledges the help of several EBSD experts in assisting and training during the data collection including Janelle Homburg, Phil Skemer, Eric Goergen and Jessica Warren. We also acknowledge the efforts of Mike Braun, Carlos Garrido and Karen Hanghoj in the sample collection and thin section making. We thank Luiz Morales for providing the J-index data for all crystallographic axes from anorthosite samples measured in Morales et al. (2011). The work strongly benefited from additional discussions with Mike Cheadle and Oliver Jagoutz. The manuscript was significantly improved by reviews from Lars Hansen and an anonymous reviewer. Work on this project over twenty years was supported by NSF-EAR grants EAR-1049905, EAR-0739010, OCE-0426160, EAR-0337677, OCE-0118572, OCE-9819666, OCE-9711170, and OCE-9416616 awarded to Kelemen, Hirth and their colleagues.

Appendix A. Supplementary material

Supplementary material related to this article can be found online at http://dx.doi.org/10.1016/j.epsl.2015.07.001.

References

Benn, K., Allard, B., 1989. Preferred mineral orientations related to magmatic flow in ophiolite layered gabbros. J. Petrol. 30, 925–946.
Bosch, D., Jamais, M., Boudier, F., Nicolas, A., Dautria, J.M., Agrinier, P., 2004. Deep and high-temperature hydrothermal circulation in the Oman ophiolite – petrological and isotopic evidence. J. Petrol. 45, 1181–1208.
Boudier, F., Nicolas, A., 2011. Axial melt lenses at oceanic ridges – a case study in the Oman ophiolite. Earth Planet. Sci. Lett. 304, 313–325.
Boudier, F., Nicolas, A., Ildefonse, B., 1996. Magma chambers in the Oman ophiolite: fed from the top and the bottom. Earth Planet. Sci. Lett. 144, 239–250.
Browning, P., 1984. Cryptic variation within the cumulate sequence of the Oman ophiolite: magma chamber depth and petrological implications. In: Gass, I.G. (Ed.), Ophiolites and Oceanic Lithosphere. Geological Society Special Publication, London.
Canales, J.P., Carton, H., Carbotte, S.M., Mutter, J.C., Nedimovic, M.R., Xu, M., Aghaei, O., Marjanovic, M., Newman, K., 2012. Network of off-axis melt bodies at the East Pacific Rise. Nat. Geosci. 5, 279–283.

Canales, J.P., Nedimovic, M.R., Kent, G.M., Carbotte, S.M., Detrick, R.S., 2009. Seismic reflection images of a near-axis melt sill within the lower crust at the Juan de Fuca ridge. Nature 460, 89–93.
Canales, J.P., Singh, S.C., Detrick, R.S., Carbotte, S.M., Harding, A., Kent, G.M., Diebold, J.B., Babcock, J., Nedimovic, M.R., 2006. Seismic evidence for variations in axial magma chamber properties along the southern Juan de Fuco Ridge. Earth Planet. Sci. Lett. 246, 353–366.
Chen, Y.J., 2001. Thermal effects of gabbro accretion from a deeper second melt lens at the fast spreading East Pacific Rise. J. Geophys. Res. 106, 8581–8588.
Cherkaoui, A.S.M., Wilcock, W.S.D., Dunn, R.A., Toomey, D.R., 2003. A numerical model of hydrothermal cooling and crustal accretion at a fast spreading mid-ocean ridge. Geochem. Geophys. Geosyst. 4.
Coogan, L.A., Jenkin, G.R.T., Wilson, R.N., 2002. Constraining the cooling rate of the lower oceanic crust: a new approach applied to the Oman ophiolite. Earth Planet. Sci. Lett. 199, 127–146.
Crawford, W.C., Webb, S.C., 2002. Variations in the distribution of magma in the lower crust and at the Moho beneath the East Pacific Rise at 9°–10°N. Earth Planet. Sci. Lett. 203, 117–130.
Detrick, R.S., Buhl, P., Vera, E., Mutter, J., Orcutt, J., Madsen, J., Brocher, T., 1987. Multichannel seismic imaging of a crustal magma chamber along the East Pacific Rise. Nature 326, 35–41.
Dunn, R.A., Toomey, D.R., Solomon, S.C., 2000. Three-dimensional seismic structure and physical properties of the crust and shallow mantle beneath the East Pacific Rise at 9 degrees 30′N. J. Geophys. Res., Solid Earth 105, 23537–23555.
Garrido, C.J., Kelemen, P.B., Hirth, G., 2001. Variation of cooling rate with depth in lower crust formed at an oceanic spreading ridge: plagioclase crystal size distributions in gabbros from the Oman ophiolite. Geochem. Geophys. Geosyst. 2.
Ghosh, S.K., Ramberg, H., 1976. Reorientation of inclusions by combination of pure shear and simple shear. Tectonophysics 34 (1), 1–70.
Gillis, K., Mével, C., Allan, J., et al., 1993. In: Proc. ODP, Init. Repts., vol. 147. Ocean Drilling Program, College Station, TX.
Gillis, K.M., Snow, J.E., Klaus, A., Abe, N., Adriao, A.B., Akizawa, N., Ceuleneer, G., Cheadle, M.J., Faak, K., Falloon, T.J., Friedman, S.A., Godard, M., Guerin, G., Harigane, Y., Horst, A.J., Hoshide, T., Ildefonse, B., Jean, M.M., John, B.E., Koepke, J., Machi, S., Maeda, J., Marks, N.E., McCaig, A.M., Meyer, R., Morris, A., Nozaka, T., Python, M., Saha, A., Wintsch, R.P., 2014. Primitive layered gabbros from fast-spreading lower oceanic crust. Nature 505, 204.
Grimes, C.B., Cheadle, M.J., John, B.E., Reiners, P.W., Wooden, J.L., 2011. Cooling rates and the depth of detachment faulting at oceanic core complexes: evidence from zircon Pb/U and (U–Th)/He ages. Geochem. Geophys. Geosyst. 12.
Han, S., Carbotte, S.M., Carton, H., Mutter, J.C., Aghaei, O., Nedimović, M.R., Canales, J.P., 2014. Architecture of on- and off-axis magma bodies at EPR 9°37–40′N and implications for oceanic crustal accretion. Earth Planet. Sci. Lett. 390, 31–44.
Hansen, L.N., Cheadle, M.J., John, B.E., Swapp, S.M., Dick, H.J.B., Tucholke, B.E., Tivey, M.A., 2013. Mylonitic deformation at the Kane oceanic core complex: implications for the rheological behavior of oceanic detachment faults. Geochem. Geophys. Geosyst. 14, 3085–3108.
Henstock, T.J., Woods, A.W., White, R.S., 1993. The accretion of oceanic crust by episodic sill intrusion. J. Geophys. Res., Solid Earth 98, 4143–4161.
Ildefonse, B., Launeau, P., Bouchez, J.L., Fernandez, A., 1992a. Effect of mechanical interactions on the development of shape preferred orientations – a 2-dimensional experimental approach. J. Struct. Geol. 14, 73.
Ildefonse, B., Sokoutis, D., Mancktelow, N.S., 1992b. Mechanical interactions between rigid particles in a deforming ductile matrix – analog experiments in simple shear-flow. J. Struct. Geol. 14, 1253–1266.
Jousselin, D., Morales, L.F.G., Nicolle, M., Stephant, A., 2012. Gabbro layering induced by simple shear in the Oman ophiolite Moho transition zone. Earth Planet. Sci. Lett. 331, 55–66.
Kelemen, P.B., Koga, K., Shimizu, N., 1997. Geochemistry of gabbro sills in the crust-mantle transition zone of the Oman ophiolite: implications for the origin of the oceanic lower crust. Earth Planet. Sci. Lett. 146, 475–488.
Korenaga, J., Kelemen, P.B., 1998. Melt migration through the oceanic lower crust: a constraint from melt percolation modeling with finite solid diffusion. Earth Planet. Sci. Lett. 156, 1–11.
Lister, G.F., 1977. Qualitative models of spreading-center processes, including hydrothermal penetration. Tectonophysics 37, 203–218.
Maclennan, J., Hulme, T., Singh, S.C., 2004. Thermal models of oceanic crustal accretion: linking geophysical, geological and petrological observations. Geochem. Geophys. Geosyst. 5.
MacLeod, C.J., Lissenberg, C.J., Bibby, L.E., 2013. "Moist MORB" axial magmatism in the Oman ophiolite: the evidence against a mid-ocean ridge origin. Geology 41, 459–462.
MacLeod, C.J., Yaouancq, G., 2000. A fossil melt lens in the Oman ophiolite: implications for magma chamber processes at fast spreading ridges. Earth Planet. Sci. Lett. 176, 357–373.
Manning, C.E., MacLeod, C.J., Weston, P.E., 2000. Lower-crustal cracking front at fast-spreading ridges: evidence from the East Pacific Rise and the Oman ophiolite. In: Dilek, Y., Moores, E.M., Elthon, D., Nicolas, A. (Eds.), Ophiolites and Oceanic Crust: New Insights from Field Studies and the Ocean Drilling Program, Boulder, CO. Spec. Pap. Geol. Soc. Am. 349, 261–272.
Marjanović, M., Carbotte, S.M., Carton, H., Nedimović, M.R., Mutter, J.C., Canales, J.P., 2014. A multi-sill magma plumbing system beneath the axis of the East Pacific Rise. Nat. Geosci. 7 (11), 825–829.
Mehl, L., Hirth, G., 2008. Plagioclase preferred orientation in layered mylonites: evaluation of flow laws for the lower crust. J. Geophys. Res., Solid Earth 113.
Mevel, C., Gillis, K.M., Allan, J.F., Meyer, P.S., 1996. In: Proc. ODP, Sci. Results, vol. 147. Ocean Drilling Program, College Station, TX.
Morales, L.F.G., Boudier, F., Nicolas, A., 2011. Microstructures and crystallographic preferred orientation of anorthosites from Oman ophiolite and the dynamics of melt lenses. Tectonics 30.
Morgan, J.P., Chen, Y.J., 1993. The genesis of oceanic crust: magma injection, hydrothermal circulation, and crustal flow. J. Geophys. Res., Solid Earth 98, 6283–6297.
Nicolas, A., Boudier, F., France, L., 2009. Subsidence in magma chamber and the development of magmatic foliation in Oman ophiolite gabbros. Earth Planet. Sci. Lett. 284, 76–87.
Nicolas, A., Boudier, F., Ceuleneer, G., 1988a. Mantle flow patterns and magma chambers at ocean ridges: evidence from the Oman ophiolite. Mar. Geophys. Res. 9, 293–310.
Nicolas, A., Reuber, I., Benn, K., 1988b. A new magma chamber model based on structural studies in the Oman ophiolite. Tectonophysics 151 (1), 87–105.
Pallister, J.S., Hopson, C.A., 1981. Samail ophiolite plutonic suite – field relations, phase variation, cryptic variation and layering, and a model of a spreading ridge magma chamber. J. Geophys. Res. 86, 2593–2644.
Pearce, J.A., Alabaster, T., Shelton, A.W., Searle, M.P., 1981. The Oman ophiolite as a cretaceous arc-basin complex – evidence and implications. Philos. Trans. R. Soc. A 300, 299.
Picard, D., Arbaret, L., Pichavant, M., Champallier, R., Launeau, P., 2011. Rheology and microstructure of experimentally deformed plagioclase suspensions. Geology 39, 747–750.
Quick, J.E., Denlinger, R.P., 1993. Ductile deformation and the origin of layered gabbro in ophiolites. J. Geophys. Res., Solid Earth 98, 14015–14027.
Rioux, M., Bowring, S., Kelemen, P., Gordon, S., Dudas, F., Miller, R., 2012. Rapid crustal accretion and magma assimilation in the Oman-UAE ophiolite: high precision U–Pb zircon geochronology of the gabbroic crust. J. Geophys. Res., Solid Earth 117.
Schmitt, A.K., Perfit, M.R., Rubin, K.H., Stockli, D.F., Smith, M.C., Cotsonika, L.A., Zellmer, G.F., Ridley, W.I., Lovera, O.M., 2011. Rapid cooling rates at an active mid-ocean ridge from zircon thermochronology. Earth Planet. Sci. Lett. 302, 349–358.
Singh, S.C., Harding, A.J., Kent, G.M., Sinha, M.C., Combier, V., Bazin, S., Tong, C.H., Pye, J.W., Barton, P.J., Hobbs, R.W., White, R.S., Orcutt, J.A., 2006. Seismic reflection images of the Moho underlying melt sills at the East Pacific Rise. Nature 442, 287–290.
Singh, S.C., Kent, G.M., Collier, J.S., Harding, A.J., Orcutt, J.A., 1998. Melt to mush variations in crustal magma properties along the ridge crest at the southern East Pacific Rise. Nature 394, 874–878.
Sinton, J.M., Detrick, R.S., 1992. Mid-ocean ridge magma chambers. J. Geophys. Res., Solid Earth 97, 197–216.
Skemer, P., Katayama, B., Jiang, Z.T., Karato, S., 2005. The misorientation index: development of a new method for calculating the strength of lattice-preferred orientation. Tectonophysics 411, 157–167.
Sleep, N.H., 1975. Formation of oceanic crust: some thermal constraints. J. Geophys. Res. 80, 4037–4042.
Smewing, J.D., 1981. Mixing characteristics and compositional differences in mantle-derived melts beneath spreading axes – evidence from cyclically layered rocks in the ophiolite of North Oman. J. Geophys. Res. 86, 2645–2659.
Spinelli, G.A., Harris, R.N., 2011. Effects of the legacy of axial cooling on partitioning of hydrothermal heat extraction from oceanic lithosphere. J. Geophys. Res., Solid Earth 116.
Teagle, D.A.H., Ildefonse, B., Blum, P., 2012. Superfast spreading rate crust 4. In: Integrated Ocean Drilling Program Expedition 335 Scientific Prospectum. In: Proc. IODP, vol. 335. Integrated Ocean Drilling Program Management International, Inc., Tokyo.
VanTongeren, J.A., Kelemen, P.B., Hanghoj, K., 2008. Cooling rates in the lower crust of the Oman ophiolite: Ca in olivine, revisited. Earth Planet. Sci. Lett. 267, 69–82.
Vera, E.E., Mutter, J.C., Buhl, P., Orcutt, J.A., Harding, A.J., Kappus, M.E., Detrick, R.S., Brocher, T., 1990. The structure of 0 to 0.2 Ma old oceanic crust at 9°N on the East Pacific Rise from expanded spread profiles. J. Geophys. Res. 95, 15529–515556.
Woodcock, N.H., 1977. Specification of fabric shapes using an eigenvalue method. Geol. Soc. Am. Bull. 88, 1231–1236.
Yaouancq, G., MacLeod, C.J., 2000. Petrofabric investigation of gabbros from the Oman ophiolite: comparison between AMS and rock fabric. Mar. Geophys. Res. 21, 289–305.
Zha, Y., Webb, S.C., Nooner, S.L., Crawford, W.C., 2014. Spatial distribution and temporal evolution of crustal melt distribution beneath the East Pacific Rise at 9°–10°N inferred from 3-D seafloor compliance modeling. J. Geophys. Res., Solid Earth 119. http://dx.doi.org/10.1002/2014JB011131.